



**HAL**  
open science

## Identification of frequency-dependent viscoelastic damped structures using an adjoint method

M. Hamdaoui, K.S. Ledi, Guillaume Robin, El Mostafa Daya

### ► To cite this version:

M. Hamdaoui, K.S. Ledi, Guillaume Robin, El Mostafa Daya. Identification of frequency-dependent viscoelastic damped structures using an adjoint method. *Journal of Sound and Vibration*, 2019, 453, pp.237-252. <10.1016/j.jsv.2019.04.022>. <hal-03036036>

**HAL Id: hal-03036036**

**<https://hal.science/hal-03036036v1>**

Submitted on 22 Oct 2021

HAL is a multi-disciplinary open access archive for the deposit and dissemination of scientific research documents, whether they are published or not. The documents may come from teaching and research institutions in France or abroad, or from public or private research centers.

L'archive ouverte pluridisciplinaire HAL, est destinée au dépôt et à la diffusion de documents scientifiques de niveau recherche, publiés ou non, émanant des établissements d'enseignement et de recherche français ou étrangers, des laboratoires publics ou privés.



Distributed under a Creative Commons CC BY-NC 4.0 - Attribution - Non-commercial use - International License

# Identification of frequency-dependent viscoelastic damped structures using an adjoint method

M. Hamdaoui, K.S.Ledi, G. Robin, E.M.Daya <sup>1</sup>

*Université de Lorraine, CNRS, Arts et Métiers ParisTech, LEM3, F-57000 Metz, France*  
Tel.: +33 3 87 31 54 05  
Fax : +33 3 87 31 53 66

---

## Abstract

Viscoelastic parameter identification in sandwich structures (shear modulus and loss factor) is addressed in the present paper. Finite element modelling of three-layered viscoelastic sandwich beams is considered leading to the resolution of a non-linear eigenvalue problem for modal properties determination. An adjoint-based gradient method is developed to minimize the quadratic error between the finite element model and the experimental modal data (frequencies and loss factors). The discrete adjoint approach requires the resolution of a linear system to compute the gradient of the objective function. The method is successfully validated in comparison with central finite difference schemes for gradient's computation. Two use cases are used to illustrate the performance of the method in the case of viscoelastic sandwich beams parameter identification.

*Keywords:* Identification, Adjoint method, Non-linear eigenvalue problem, Viscoelastic, Sandwich structure

---

## 1. Introduction

Constrained viscoelastic structures (CVS) are commonly used for noise and vibration control. They are usually composed of a viscoelastic layer sandwiched between two stiff layers. In the literature many works have been devoted to study the vibrational characteristics of viscoelastic damped sandwich structures. Rao [1] proposed a semi-analytical method to compute resonant frequencies and loss factors for three-layered beams. Soni [2] developed a finite elements computer program Magna-D to compute frequencies, damping ratios and response frequency curves of frequency dependent viscoelastic structures. Johnson and Kienholz [3] used volumic finite elements along with modal strain energy method to determine modal frequencies, damping ratios and frequency response curves of frequency dependent viscoelastic structures. Ma and He [4] employed finite element analysis associated with an asymptotic solution method using Padé approximants to predict damping ratios and frequencies of viscoelastic sandwich plates. Daya and Potier-Ferry [5] used finite elements and an asymptotic numerical method to determine frequencies and damping ratios of frequency dependent viscoelastic sandwich structures. Chen *et al.* [6] proposed an order-reduction iterative algorithm to solve the non-linear eigenvalue problem arising in modal analysis of viscoelastic sandwich

---

<sup>1</sup>Since 1880.

15 structures using finite elements. Bilasse *et al.* [7] developed a finite elements based numerical method for linear and non linear vibrations analysis of viscoelastic sandwich structures. Moita *et al.* [8] established a finite element model framework for vibration analysis of active-passive damped multilayer sandwich plates. Akoussan *et al.* [9] detailed a finite element model for laminated viscoelastic sandwich structures. Recently, Zghal *et al.*[10] proposed a finite elements based reduced order model in frequency and time domains for  
20 viscoelastic sandwich structures. As the performance of CVS is highly dependent on the characteristics of the viscoelastic layer, it is important to characterize it accurately. In the literature, many methods have been proposed so far to identify viscoelastic materials properties. Most of them rely on experimental tests and a viscoelastic model fit. In the time domain, creep and relaxation tests (constant stress and strain uniaxial experiments, respectively) [11] are generally used to fit a viscoelastic model. A procedure based on creep  
25 tests and least square error minimization (between measured and model based creep moduli) to characterize a three-parameter viscoelastic fractional model is proposed in [12]. Least square fitting algorithms for Dirichlet-Prony series representation of creep data is presented in [13]. Several identification methods for force and displacement temporal data using hysteresis loop and error functional minimization are presented in [14]. On the other side, in the frequency domain, the most well known method is certainly the dynamical  
30 mechanical analysis (DMA) that consists in applying harmonic loadings to determine the complex Young modulus [15]. Later on, a method to find the parameters of a generalized Maxwell model from experimental storage and loss moduli data is described in [16]. A least square procedure to fit a generic complex parameters model for viscoelastic complex modulus to experimental data is detailed in [17]. Graphical methods and Newton-Raphson procedures to fit complex moduli by rational fractions and fractional derivative models using experimental data is detailed in [18]. A method to identify a five parameter fractional derivative  
35 model using its properties around the maximum loss factor is introduced in [19]. New graphical methods relying on the TIBI diagram to identify the parameters of fractional derivatives models is presented in [20]. A robust method to determine the parameters of a generalized Maxwell model is proposed in [21]. The Kramers-Kronig relationships are used in [22] to characterize the temperature and frequency viscoelastic  
40 behaviour of Deltane using DMA tests along with a least square fitting procedure with different viscoelastic models. Other methods aim at characterizing the viscoelastic material while being embedded in a structure such as CVS. The Oberst method described in [23] consists in performing a series of vibration tests on a constrained or unconstrained viscoelastic beam in order to obtain frequency response curves (FRF). Then, modal frequencies and loss factors are determined using either the  $-3$  dB bandwidth or the Nyquist diagram  
45 methods [24]. The material Young modulus and loss factor are usually obtained using the Ross-Kerwin-Ungar (RKU) relationships [25],[26]. When no analytical relationship (such as the RKU relationships) is available, computational models could be used. A method based on minimizing the difference between measured and computed finite elements frequency response curves (FRF) using a gradient based optimization algorithm to identify the parameters of a fractional derivative model is proposed in [27]. Furthermore, [28]  
50 used a response surface methodology, finite element modelling and simple vibrations tests to characterize the viscoelastic properties of sandwich beams with ISD112 cores. On the other side, [29] used finite element

modelling and gradient-based optimization to fit a generalized Maxwell model to experimental modal data. The gradient of the relative error between modal experimental data coming from vibration tests and finite element numerical model predictions was computed by means of automatic differentiation. In addition to that, [30] determined a fractional derivative model for viscoelastic sandwich beams by minimizing the error between predicted and measured frequency response curves (FRF) at specified control frequencies. Sandwich beams shear complex moduli is identified in [31] using the force analysis technique with homogenization and Timoshenko beam's theory. More recently, [32] used the response surface methodology, a simplified FRF representation and an optimization approach to identify the frequency dependent mechanical parameter of unconstrained viscoelastic plates. An iterative method based on Rayleigh quotient to identify the viscoelastic properties of damped sandwich beams has also been proposed in [33]. The aim of this article is to present an adjoint method for gradient computation of the error between modal experimental data and a numerical model relying on finite elements [34]. Many methods have been proposed so far in the literature to compute the gradient of numerical objective functions [35]. One can cite finite differences methods [36], complex step methods [37], automatic differentiation methods [38], direct differentiation methods and adjoint methods [39]. Adjoint methods come from the field of optimal control [40, 41]. They have been extended to the field of partial derivative equations by the seminal work of Jacques Louis-Lions [42]. They are popular in many engineering fields such as topology optimization [43, 44], shape optimization [45], optimal design in computational fluid dynamics [46], optimal flow control [47] and parameter identification [48, 49, 50]. Their main advantage relies on computing the gradient of an objective function thanks to the resolution of a linear adjoint equation. In the present paper, we present a discrete adjoint approach for gradient computation when the state equations are described by a non linear eigenvalue problem. The organization of the paper is as follows. In section 2, the finite element model is detailed. In section 3, the adjoint state method for gradient computation is derived. In section 4, the identification process is presented. In section 5, two use cases are used to illustrate the use of the method.

## 2. Finite element model

### 2.1. Visco-elastic sandwich model

A symmetric rectangular cross-section sandwich beam is considered. The viscoelastic layer is located between two elastic layers (see Fig. 1). The symbols  $x$ ,  $y$  and  $z$  denote respectively the coordinates along the length, the width and the thickness. The symbol  $z_i$  represents the  $i^{th}$  middle plane coordinate with respect to  $z = 0$ . The subscripts  $i = 1$  or  $i = 3$  refer to the elastic faces while the subscript  $i = 2$  refers to the core layer. The thickness of the elastic face layer is  $h_f$  and the thickness of the visco-elastic core is  $h_c$ . The beam length in  $x$  direction is  $L$  while the width in  $y$  direction is  $b$ . The damping of the structure is due to the shearing in the visco-elastic core layer. It is assumed that :

- plane transverse sections to the middle plane remain plane after bending,
- the three layers undergo the same transverse deflection,

- shear strain is neglected in the elastic layers,
- no slipping occurs at the interfaces between the three layers,
- the constitutive materials of the beam are linear, homogeneous and isotropic.

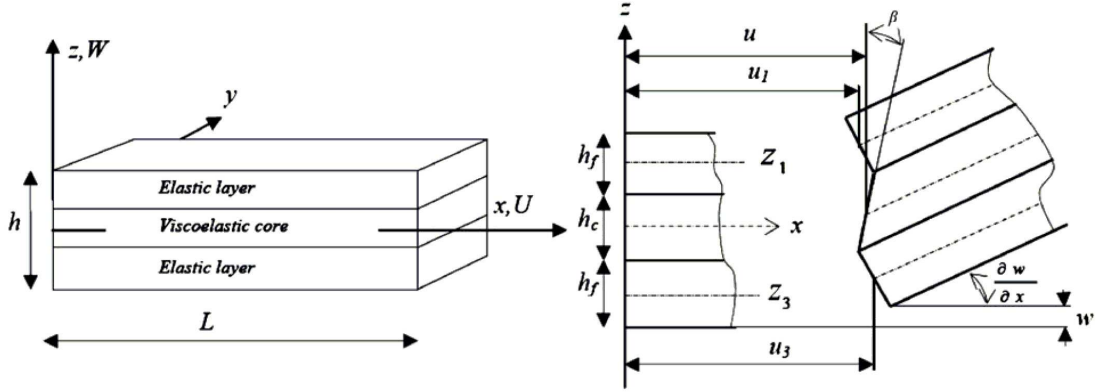


Figure 1: Sandwich beam sketch

90 Euler-Bernoulli's beam theory is used for the elastic layers and the Timoshenko's beam theory is employed for the visco-elastic layer. However, the choice of these kinematics show limitations in certain cases. Hu *et al.* [51] evaluated classical zig-zag models through static and dynamic tests. They showed that if  $\frac{h_c}{h_f} \leq 10$ , these models remain accurate. In this study, this condition holds. The core material is linearly visco-elastic with a complex frequency dependent shear modulus  $G^*(\omega)$ , but the Poisson's ratio  $\nu_c$  is assumed to be real and constant.

95 Based on these assumptions, the strain, the displacement fields and the constitutive laws governing the viscoelastic sandwich beam motion can be derived. Following the notation of Fig. 1 the normal strain  $\epsilon_i$  and the displacement  $(U_i, W_i)$  fields are presented for the elastic layers  $i = 1, 3$  as follows :

$$U_i(x, z, t) = u_i(x, t) - (z - z_i) \frac{\partial w}{\partial x}, \quad (1)$$

$$W_i(x, z, t) = w(x, t), \quad (2)$$

$$\epsilon_i(x, z, t) = \frac{\partial u_i}{\partial x} - (z - z_i) \frac{\partial^2 w}{\partial x^2}, \quad (3)$$

100 where  $z_1 = \frac{h_f + h_c}{2} = -z_3$ ,  $u_i$  represents the axial displacement of the middle surface of the  $i^{th}$  layer and  $w$  denotes the common transverse displacement. The quantities related to the viscoelastic layer  $i = 2$  are given by:

$$U_2(x, z, t) = u(x, t) + z\beta, \quad (4)$$

$$W_2(x, z, t) = w(x, t), \quad (5)$$

$$\epsilon_2(x, z, t) = \frac{\partial u}{\partial x} + z \frac{\partial \beta}{\partial x}, \quad (6)$$

$$\xi_2 = \beta + \frac{\partial w}{\partial x}, \quad (7)$$

where  $\xi_2$  is the shear strain. The continuity of the displacement field at layers interfaces gives :

$$u_1 = u + \left(\frac{h_c}{2}\beta - \frac{h_f}{2}\frac{\partial w}{\partial x}\right), \quad (8)$$

$$u_3 = u - \left(\frac{h_c}{2}\beta - \frac{h_f}{2}\frac{\partial w}{\partial x}\right). \quad (9)$$

Then, the generalized displacement vector  $u, w, \beta$  related to the core layer could be defined. The generalized Hooke's stress-strain law gives for the axial force  $N_i$  and bending moment  $M_i$  of each layer  $i = 1, 3$  :

$$N_i(x, t) = E_f S_f \frac{\partial u_i}{\partial x}, \quad (10)$$

$$M_i(x, t) = E_f I_f \frac{\partial^2 w}{\partial x^2}, \quad (11)$$

105 where  $E_f$  is the Young's modulus of the elastic faces,  $S_f$  and  $I_f$  are respectively the area and the quadratic moment of the elastic faces cross-section. The axial force and bending moment for the visco-elastic layer are given by

$$N_2(x, t) = S_c Y(t) * \frac{\partial}{\partial t} \left(\frac{\partial u}{\partial x}\right), \quad (12)$$

$$M_2(x, t) = I_c Y(t) * \frac{\partial}{\partial t} \left(\frac{\partial \beta}{\partial x}\right), \quad (13)$$

$$T(x, t) = \frac{S_c}{2(1 + \nu_c)} Y(t) * \frac{\partial}{\partial t} \left(\beta + \frac{\partial w}{\partial x}\right), \quad (14)$$

where  $S_c$  and  $I_c$  are the area and quadratic moment of the cross-section of the visco-elastic core,  $Y(t)$  is the visco-elastic relaxation function,  $\nu_c$  is the Poisson's ratio and  $T$  is the shear stress. The virtual work principle is used to establish the equation of motion of the visco-elastic sandwich beam. The transverse inertia effects are considered, however, the longitudinal and rotary inertia effects are neglected [34]. The three components of the virtual work principles are

$$\delta P_{int} = - \int_0^L (N \delta u_{,x} + M_\beta \delta \beta_{,x} + M_w \delta w_{,xx} + T(\delta w_{,x} + \delta \beta)) dx, \quad (15)$$

$$\delta P_{ext} = 0, \quad (16)$$

$$\delta P_{acc} = \int_0^L (2\rho_f S_f + \rho_c S_c) w_{,tt} \delta w dx, \quad (17)$$

where  $\rho_f$  and  $\rho_c$  are the mass density of the elastic faces and the mass density of the visco-elastic layer, respectively. The symbols  $\delta u$ ,  $\delta w$  and  $\delta \beta$  represent the components of the virtual displacement vector.

115 Furthermore,  $N$ ,  $M_\beta$  and  $M_w$  are defined by

$$N = N_1 + N_2 + N_3, \quad (18)$$

$$M_\beta = M_2 + (N_1 - N_3) \frac{h_c}{2}, \quad (19)$$

$$M_w = M_1 + M_3 + (N_3 - N_1) \frac{h_f}{2}. \quad (20)$$

The equation of motion is then given by

$$\int_0^L (N \delta u_{,x} + M_\beta \delta \beta_{,x} + M_w \delta w_{,xx} + T(\delta w_{,x} + \delta \beta)) dx = - \int_0^L (2\rho_f S_f + \rho_c S_c) w_{,tt} \delta w dx. \quad (21)$$

Since the axial inertia terms are not considered here, the axial equilibrium could be obtained by

$$\int_0^L N \delta u_{,x} = 0, \quad (22)$$

and the transverse equation of motion could then be given by:

$$\int_0^L (M_\beta \delta \beta_{,x} + M_w \delta w_{,xx} + T(\delta w_{,x} + \delta \beta)) dx = - \int_0^L (2\rho_f S_f + \rho_c S_c) w_{,tt} \delta w dx. \quad (23)$$

The finite element method is used in the following to solve equation (23) since no analytical solution exist.

## 2.2. Finite element formulation

The equation of motion is sought in the following harmonic form :

$$w(x,t) = W(x) \exp(i\omega t), \quad (24)$$

$$\beta(x,t) = B(x) \exp(i\omega t). \quad (25)$$

One dimensional two nodes finite element is used in this work. Each node has three degrees of freedom : the transverse displacement  $W$ , the slope  $W_{,x}$  and the rotation  $B$ . Thus for each element bounded with the nodes 1 and 2, the nodal displacement vector is

$$\mathbf{U}^e = [W_1, W_{1,x}, B_1, W_2, W_{2,x}, B_2]^T. \quad (26)$$

Using polynomial shape functions, the displacement field is written as follows

$$[\mathbf{WB}]^T = [\mathbf{N}_w, \mathbf{N}_\beta]^T \mathbf{U}^e, \quad (27)$$

where

$$\mathbf{N}_w = [n_1(\xi), n_2(\xi), 0, n_3(\xi), n_4(\xi), 0], \quad (28)$$

$$\mathbf{N}_\beta = [0, 0, n_5(\xi), 0, 0, n_6(\xi)], \quad (29)$$

120 and  $\xi = \frac{2x}{L^e} - 1$  with  $L^e$  the length of the one dimensional element and  $x$  the real spatial variable  $\in [0, L^e]$ .

The shape functions are given by:

$$n_1(\xi) = \frac{(1-\xi)^2(2+\xi)}{2}, \quad (30)$$

$$n_2(\xi) = \frac{L^e(1-\xi)^2(1+\xi)}{8}, \quad (31)$$

$$n_3(\xi) = \frac{(1+\xi)^2(2-\xi)}{4}, \quad (32)$$

$$n_4(\xi) = -\frac{L^e(1+\xi)^2(1-\xi)}{8}, \quad (33)$$

$$n_5(\xi) = \frac{1-\xi}{2}, \quad (34)$$

$$n_6(\xi) = \frac{1+\xi}{2}. \quad (35)$$

Finally, by inserting equations (24)-(35) into the equations of motion , one obtains the following non-linear complex eigenvalue problem

$$(\mathbf{K}_0 + G^*(\omega)\mathbf{K}_v - \omega^2\mathbf{M})\mathbf{U} = 0, \quad (36)$$

where  $\mathbf{M}$ ,  $\mathbf{K}_0$  and  $\mathbf{K}_v$  are the global mass, elastic and viscoelastic stiffness matrices and  $\mathbf{U}$  is the generalized displacement vector. The matrix formulation (36) of the visco-elastic sandwich beam in free vibrations is well-known [52]. Many methods have been used to solve the resulting non-linear eigenvalue problem (36) taking into account the frequency dependence of the visco-elastic shear modulus. Several methods such as the direct frequency response method [2], the iterative shift-invert method [8], the order-reduction iterative algorithm [6], the high-order sensitivity method [53], the asymptotic numerical method [52], the inverse iteration [54], the non-linear Arnoldi/Jacobi-Davidson methods [55, 56] have been proposed to tackle this problem. Recently, Hamdaoui *et al.* [57] proposed a comparison of such methods in the context of viscoelastic laminated plates.

### 2.3. Eigenmodes computation using inverse iteration

The problem (36) can be rewritten as

$$\mathbf{T}(\lambda)\mathbf{X} = 0 \quad (37)$$

by letting  $\lambda = \omega^2$ ,  $\mathbf{X} = \mathbf{U}$  and  $\mathbf{T}$  a parameter dependent complex valued matrix. The complex eigenmodes and eigenvalues are computed exactly using the method of the inverse iteration.

*Inverse iteration (IV).* The inverse iteration [54] is based on applying Newton's method to the system formed by (36) and an orthogonalization condition as follows

$$\begin{aligned} \mathbf{T}(\lambda)\mathbf{X} &= 0, \\ \mathbf{Z}^H \mathbf{X} &= 1, \end{aligned} \quad (38)$$

where  $\mathbf{Z}$  is a normalized vector. At step  $k$  of the algorithm, one can compute  $\lambda^{k+1}$  and  $\mathbf{X}^{k+1}$  using the two following update equations:

$$\begin{aligned} \mathbf{T}(\lambda^k)\mathbf{X}^{k+1} &= \frac{\partial \mathbf{T}}{\partial \lambda}(\lambda^k)\mathbf{X}^k, \\ \lambda^{k+1} &= \lambda^k - \frac{\mathbf{Z}^H \mathbf{X}^k}{\mathbf{Z}^H \mathbf{X}^{k+1}}, \end{aligned}$$

where  $(\lambda^{k+1}, \mathbf{X}^{k+1})$  are current iterates. At each iteration, this algorithm involves the inversion of a matrix which can be very costly, therefore it could be only used to solve small sized non-linear eigenvalue problems. In the present work, we use  $\mathbf{Z} = \mathbf{X}^k$  and initialized the process by  $(\mathbf{X}_0^i, \lambda_0^i)$  (solutions to the real generalized linear eigenvalue problem obtained by setting  $G^*(\omega) = 0$  in (36)) to find the eigenvalue number  $i$  and its corresponding eigenvector. It is worth mentioning that  $\mathbf{T}(\lambda)$  becomes singular in the vicinity of the target eigenvalue as  $\det(\mathbf{T}(\lambda))$  becomes exactly zero and the matrix is no longer invertible. Then, the algorithm is stopped when the matrix becomes singular since the iterates are very close to the eigenvalue. The main steps

<p><b>Data:</b> Approximate eigenvalue <math>\lambda_0</math>, Approximate eigenvector <math>X_0</math>, <math>\epsilon_{tol}</math></p> <p><b>Result:</b> <math>X</math> and <math>\lambda</math></p> <ol style="list-style-type: none"> <li>1 Initialize: <math>X^0 = \frac{X_0}{\ X_0\ }</math>, <math>\lambda^0 = \lambda_0</math>;</li> <li>2 <b>while</b> <math>\frac{\ r\ }{\ X^k\ } &lt; \epsilon_{tol}</math> <b>do</b></li> <li>3     Solve for <math>X^{k+1}</math>, <math>T(\lambda^k)X^{k+1} = \frac{\partial T}{\partial \lambda}(\lambda^k)X^k</math>;</li> <li>4     Compute <math>\lambda^{k+1} = \lambda^k - \frac{(X^k)^H X^k}{(X^k)^H X^{k+1}}</math>;</li> <li>5     Normalize <math>X^{k+1}</math>, <math>X^{k+1} = \frac{X^{k+1}}{(X^k)^H X^{k+1}}</math>;</li> <li>6     Compute the residual <math>r = T(\lambda^{k+1})X^{k+1}</math>;</li> <li>7     Increment <math>k</math>, <math>k = k + 1</math>;</li> <li>8 <b>end</b></li> </ol>
---

**Algorithm 1:** Inverse iteration algorithm

of the algorithm are summarized in Algorithm 1. The real frequency  $f$  and the loss factor  $\eta$  are computed by the following relationships:

$$f = \frac{\text{Re}\{\lambda\}^{\frac{1}{2}}}{2\pi}, \quad (39)$$

$$\eta = \frac{\text{Im}\{\lambda\}}{\text{Re}\{\lambda\}}. \quad (40)$$

### 3. Adjoint state method

#### 3.1. Optimization problem setup

We are interested in constrained optimization problems involving a real valued scalar function  $f(\mathbf{x}, \lambda, \mathbf{p})$  that defines a mapping from  $\mathbb{C}^n \times \mathbb{C} \times \mathbb{R}^k$  to  $\mathbb{R}$  and an equality constraint in the form of a non linear eigenvalue problem  $\mathbf{T}(\lambda, \mathbf{p})\mathbf{x} = 0$ ,  $\mathbf{x}^H \mathbf{w} = 1$ , where  $\mathbf{w} \in \mathbb{C}^n$  and  $\mathbf{T} \in \mathbf{M}_n(\mathbb{C})$ . The quantities  $(\mathbf{x}, \lambda)$  are called the state variables and  $\mathbf{p}$  is the vector of design parameters. The optimization problem can be written as follows

$$\begin{aligned} \min_{(\mathbf{x}, \lambda, \mathbf{p}) \in \mathbb{C}^n \times \mathbb{C} \times \Omega} & f(\mathbf{x}, \lambda, \mathbf{p}) \\ \text{s.t. } & \mathbf{T}(\lambda, \mathbf{p})\mathbf{x} = 0, \\ & \mathbf{x}^H \mathbf{w} = 1, \end{aligned} \quad (41)$$

with  $\Omega$  an open set of  $\mathbb{R}^k$ . It is worth noticing that this problem is equivalent to the following optimization problem

$$\min_{\mathbf{p} \in \Omega} f(\mathbf{X}(\mathbf{p}), \Lambda(\mathbf{p}), \mathbf{p}), \quad (42)$$

$\mathbf{X}(\mathbf{p})$  and  $\Lambda(\mathbf{p})$  are solutions of the non-linear equation  $\mathbf{T}(\Lambda(\mathbf{p}), \mathbf{p})\mathbf{X}(\mathbf{p}) = 0$  and  $\mathbf{X}(\mathbf{p})^H \mathbf{w} = 1$  [39]. Since the constraints are complex, they should be re-written in  $\mathbb{R}$  to be compatible with the theory of constrained

optimization. We reformulate the problem (41) as follows

$$\begin{aligned}
& \min_{(\mathbf{x}_1, \mathbf{x}_2, \lambda_1, \lambda_2, \mathbf{p}) \in \mathbb{R}^n \times \mathbb{R}^n \times \mathbb{R} \times \mathbb{R} \times \Omega} f(\mathbf{x}_1, \mathbf{x}_2, \lambda_1, \lambda_2, \mathbf{p}) \\
\text{s.t. } & \mathbf{T}_1(\lambda_1, \lambda_2, \mathbf{p})\mathbf{x}_1 - \mathbf{T}_2(\lambda_1, \lambda_2, \mathbf{p})\mathbf{x}_2 = 0, \\
& \mathbf{T}_1(\lambda_1, \lambda_2, \mathbf{p})\mathbf{x}_2 + \mathbf{T}_2(\lambda_1, \lambda_2, \mathbf{p})\mathbf{x}_1 = 0, \\
& \mathbf{w}_1^T \mathbf{x}_1 + \mathbf{w}_2^T \mathbf{x}_2 = 1, \\
& \mathbf{w}_1^T \mathbf{x}_2 - \mathbf{w}_2^T \mathbf{x}_1 = 0,
\end{aligned} \tag{43}$$

with  $(\mathbf{T}_1, \mathbf{T}_2) \in \mathbf{M}_n(\mathbb{C}) \times \mathbf{M}_n(\mathbb{C})$  such that

$$\begin{aligned}
\mathbf{x} &= \mathbf{x}_1 + i\mathbf{x}_2, \\
\mathbf{w} &= \mathbf{w}_1 + i\mathbf{w}_2, \\
\lambda &= \lambda_1 + i\lambda_2, \\
\mathbf{T} &= \mathbf{T}_1 + i\mathbf{T}_2,
\end{aligned} \tag{44}$$

where  $i$  is the complex imaginary number such that  $i^2 = -1$ .

### 3.2. First order optimality conditions

160 The Lagrangian function of the problem is defined as follows

$$\begin{aligned}
\mathcal{L}(\mathbf{x}_1, \mathbf{x}_2, \lambda_1, \lambda_2, \mathbf{p}, \boldsymbol{\xi}_1, \boldsymbol{\xi}_2, \mu_1, \mu_2) &= f(\mathbf{x}, \lambda, \mathbf{p}) \\
&+ \boldsymbol{\xi}_1^T (\mathbf{T}_1(\lambda_1, \lambda_2, \mathbf{p})\mathbf{x}_1 - \mathbf{T}_2(\lambda_1, \lambda_2, \mathbf{p})\mathbf{x}_2) \\
&+ \boldsymbol{\xi}_2^T (\mathbf{T}_1(\lambda_1, \lambda_2, \mathbf{p})\mathbf{x}_2 + \mathbf{T}_2(\lambda_1, \lambda_2, \mathbf{p})\mathbf{x}_1) \\
&+ \mu_1 (\mathbf{w}_1^T \mathbf{x}_1 + \mathbf{w}_2^T \mathbf{x}_2 - 1) + \mu_2 (\mathbf{w}_1^T \mathbf{x}_2 - \mathbf{w}_2^T \mathbf{x}_1),
\end{aligned} \tag{45}$$

where the adjoint state variables satisfy  $(\boldsymbol{\xi}_1, \boldsymbol{\xi}_2, \mu_1, \mu_2) \in \mathbb{R}^n \times \mathbb{R}^n \times \mathbb{R} \times \mathbb{R}$ . It is worth mentioning that the symbol  $\partial$  stands for a partial derivative and the symbol  $d$  represents a total derivative in what follows.

#### 3.2.1. State equations

165 The equations satisfied by the state variables are obtained by imposing the stationarity of the Lagrangian in the adjoint state variables as follows

$$\begin{aligned}
\forall i \in [1, 2], \quad \frac{\partial \mathcal{L}}{\partial \boldsymbol{\xi}_i} &= 0, \\
\forall i \in [1, 2], \quad \frac{\partial \mathcal{L}}{\partial \mu_i} &= 0,
\end{aligned} \tag{46}$$

which gives

$$\begin{aligned}\mathbf{T}(\lambda, \mathbf{p})\mathbf{x} &= 0, \\ \mathbf{w}^H \mathbf{x} &= 1,\end{aligned}\tag{47}$$

that corresponds to the original non linear eigenvalue problem.

### 3.2.2. Adjoint State equations

The equations for the adjoint state variables are given by imposing the stationarity of the Lagrangian in the state variables  $(\mathbf{x}, \lambda)$  which leads to the following system

$$\begin{aligned}\forall i \in [1, 2], \quad \frac{\partial \mathcal{L}}{\partial \mathbf{x}_i} &= 0, \\ \forall i \in [1, 2], \quad \frac{\partial \mathcal{L}}{\partial \lambda_i} &= 0,\end{aligned}\tag{48}$$

that becomes

$$\begin{aligned}\forall i \in [1, 2], \quad \frac{\partial f}{\partial \lambda_i} + \boldsymbol{\xi}_1^T \left[ \frac{\partial \mathbf{T}_1}{\partial \lambda_i} \mathbf{x}_1 - \frac{\partial \mathbf{T}_2}{\partial \lambda_i} \mathbf{x}_2 \right] + \boldsymbol{\xi}_2^T \left[ \frac{\partial \mathbf{T}_1}{\partial \lambda_i} \mathbf{x}_2 + \frac{\partial \mathbf{T}_2}{\partial \lambda_i} \mathbf{x}_1 \right] &= 0, \\ \forall i \in [1, 2], \quad \frac{\partial f}{\partial \mathbf{x}_i} + \boldsymbol{\xi}_1^T [\mathbf{T}_1 \delta_{i1} - \mathbf{T}_2 \delta_{i2}] + \boldsymbol{\xi}_2^T [\mathbf{T}_2 \delta_{i1} + \mathbf{T}_1 \delta_{i2}] \\ + \mu_1 [\mathbf{w}_1^T \delta_{i1} + \mathbf{w}_2^T \delta_{i2}] + \mu_2 [-\mathbf{w}_2^T \delta_{i1} + \mathbf{w}_1^T \delta_{i2}] &= 0,\end{aligned}\tag{49}$$

where  $\delta_{ij}$  is Kronecker's delta. We suppose that  $\lambda \mapsto \mathbf{T}(\lambda)$  is an holomorphic function, which gives us the following relationship between  $\mathbf{T}_1$  and  $\mathbf{T}_2$

$$\frac{\partial \mathbf{T}_1}{\partial \lambda_1} = \frac{\partial \mathbf{T}_2}{\partial \lambda_2}\tag{50}$$

$$\frac{\partial \mathbf{T}_1}{\partial \lambda_2} = -\frac{\partial \mathbf{T}_2}{\partial \lambda_1}.\tag{51}$$

In matrix form, the equation (49) for the adjoint state variables can be written as follows

$$\begin{bmatrix} \mathbf{T}_1^T & \mathbf{T}_2^T & \mathbf{w}_1 & -\mathbf{w}_2 \\ -\mathbf{T}_2^T & \mathbf{T}_1^T & \mathbf{w}_2 & \mathbf{w}_1 \\ \left[ \frac{\partial \mathbf{T}_1}{\partial \lambda_1} \mathbf{x}_1 + \frac{\partial \mathbf{T}_1}{\partial \lambda_2} \mathbf{x}_2 \right]^T & \left[ -\frac{\partial \mathbf{T}_1}{\partial \lambda_2} \mathbf{x}_1 + \frac{\partial \mathbf{T}_1}{\partial \lambda_1} \mathbf{x}_2 \right]^T & 0 & 0 \\ \left[ \frac{\partial \mathbf{T}_1}{\partial \lambda_2} \mathbf{x}_1 - \frac{\partial \mathbf{T}_1}{\partial \lambda_1} \mathbf{x}_2 \right]^T & \left[ \frac{\partial \mathbf{T}_1}{\partial \lambda_1} \mathbf{x}_1 + \frac{\partial \mathbf{T}_1}{\partial \lambda_2} \mathbf{x}_2 \right]^T & 0 & 0 \end{bmatrix} \begin{bmatrix} \boldsymbol{\xi}_1 \\ \boldsymbol{\xi}_2 \\ \mu_1 \\ \mu_2 \end{bmatrix} = - \begin{bmatrix} \frac{\partial f}{\partial \mathbf{x}_1} \\ \frac{\partial f}{\partial \mathbf{x}_2} \\ \frac{\partial f}{\partial \lambda_1} \\ \frac{\partial f}{\partial \lambda_2} \end{bmatrix}.\tag{52}$$

One can notice that the system of equations (52) depends on the state variables  $(\mathbf{x}, \lambda)$  that have to be determined before solving (52).

### 3.3. Gradient computation

The computation of the gradient of the objective function  $f$  could be performed by noticing that  $\forall \mathbf{p} \in \mathbb{R}^k$   $\mathbf{X}(\mathbf{p}) = \mathbf{X}_1(\mathbf{p}) + i \mathbf{X}_2(\mathbf{p})$  and  $\Lambda(\mathbf{p}) = \Lambda_1(\mathbf{p}) + i \Lambda_2(\mathbf{p})$  satisfy the state equations (46),(47) and  $\Xi_1(\mathbf{p}), \Xi_2(\mathbf{p}), M_1(\mathbf{p}), M_2(\mathbf{p})$  satisfy the adjoint equations (46),(49). Then

$$\begin{aligned} & \frac{d\mathcal{L}}{d\mathbf{p}}(\mathbf{X}_1(\mathbf{p}), \mathbf{X}_2(\mathbf{p}), \Lambda_1(\mathbf{p}), \Lambda_2(\mathbf{p}), \mathbf{p}, \Xi_1(\mathbf{p}), \Xi_2(\mathbf{p}), M_1(\mathbf{p}), M_2(\mathbf{p})) \\ &= \\ & \frac{\partial \mathcal{L}}{\partial \mathbf{p}}(\mathbf{X}_1(\mathbf{p}), \mathbf{X}_2(\mathbf{p}), \Lambda_1(\mathbf{p}), \Lambda_2(\mathbf{p}), \mathbf{p}, \Xi_1(\mathbf{p}), \Xi_2(\mathbf{p}), M_1(\mathbf{p}), M_2(\mathbf{p})), \end{aligned} \quad (53)$$

180 due to (48) and (46). Moreover,

$$\begin{aligned} & \mathcal{L}(\mathbf{X}_1(\mathbf{p}), \mathbf{X}_2(\mathbf{p}), \Lambda_1(\mathbf{p}), \Lambda_2(\mathbf{p}), \mathbf{p}, \Xi_1(\mathbf{p}), \Xi_2(\mathbf{p}), M_1(\mathbf{p}), M_2(\mathbf{p})) \\ &= \\ & f(\mathbf{X}_1(\mathbf{p}), \mathbf{X}_2(\mathbf{p}), \Lambda_1(\mathbf{p}), \Lambda_2(\mathbf{p}), \mathbf{p}), \end{aligned} \quad (54)$$

since the state equation (47) is satisfied. Then taking the derivative of (54) versus the design vector parameter  $\mathbf{p}$ , one obtains that  $\frac{df}{d\mathbf{p}} = \frac{d\mathcal{L}}{d\mathbf{p}} = \frac{\partial \mathcal{L}}{\partial \mathbf{p}}(\mathbf{X}_1(\mathbf{p}), \mathbf{X}_2(\mathbf{p}), \Lambda_1(\mathbf{p}), \Lambda_2(\mathbf{p}), \mathbf{p}, \Xi_1(\mathbf{p}), \Xi_2(\mathbf{p}), M_1(\mathbf{p}), M_2(\mathbf{p}))$  owing to (53). Finally, the gradient of the objective function  $\mathbf{G} = [G_i]_{1 \leq i \leq k}$  relatively to the vectors of parameters  $\mathbf{p} = [p_i]_{1 \leq i \leq k}$  can be expressed as follows:

$$\begin{aligned} G_i &= \frac{\partial f}{\partial p_i}(\mathbf{X}(\mathbf{p}), \Lambda(\mathbf{p}), \mathbf{p}) + \Xi_1(\mathbf{p})^T \left( \frac{\partial \mathbf{T}_1}{\partial p_i}(\Lambda_1(\mathbf{p}), \Lambda_2(\mathbf{p}), \mathbf{p}) \mathbf{X}_1(\mathbf{p}) - \frac{\partial \mathbf{T}_2}{\partial p_i}(\Lambda_1(\mathbf{p}), \Lambda_2(\mathbf{p}), \mathbf{p}) \mathbf{X}_2(\mathbf{p}) \right) \\ &+ \Xi_2(\mathbf{p})^T \left( \frac{\partial \mathbf{T}_1}{\partial p_i}(\Lambda_1(\mathbf{p}), \Lambda_2(\mathbf{p}), \mathbf{p}) \mathbf{X}_2(\mathbf{p}) + \frac{\partial \mathbf{T}_2}{\partial p_i}(\Lambda_1(\mathbf{p}), \Lambda_2(\mathbf{p}), \mathbf{p}) \mathbf{X}_1(\mathbf{p}) \right). \end{aligned} \quad (55)$$

185 In substance, for a given vector of design parameters  $\mathbf{p}$ , one has to solve the state equations (47) and the system of adjoint equations (49) to compute the gradient of the objective function.

## 4. Identification process

### 4.1. Experimental setup

A three layered viscoelastic sandwich beam with a dielectric resin is considered. The characteristics of the viscoelastic beam are given in Table 1. The experimental setup (see Fig. 2) is composed of a shaker, a laser vibrometer and a sandwich beam. The shaker generates vibrations restrained by a controller device (UCON system). Frequency excitation range is between 4 and 1500 Hz. The shaker's vibration amplitude is controlled thanks to an accelerometer (PCB Piezotronics - 352C33). The shaker's amplitude is chosen to minimize nonlinear vibrations ( $\sim 0,02$  mm displacement between 5 and 157,5Hz and a 1g acceleration between 157,5 and 1500Hz). The beam's vibration amplitude is measured by a laser vibrometer pointed on

195

Table 1: Characteristics of the viscoelastic beam

Young's modulus $E_f$	69 GPa
Poisson's ratios $\nu_c/\nu_f$	0.3 GPa
Density $\rho_f$	2766 Kg/m <sup>3</sup>
Density $\rho_c$	1550 Kg/m <sup>3</sup>
$h_c$	1 mm
$h_f$	1 mm
$L$	462 mm
$b$	30 mm

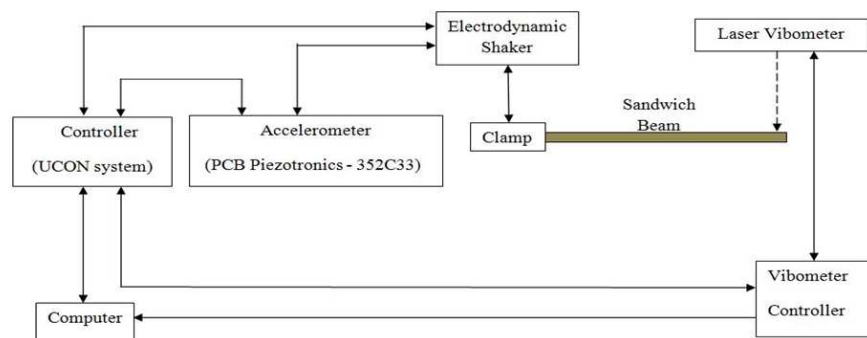


Figure 2: Experimental setup to measure resonant frequencies and loss factors of sandwich beams

its free extremity. The boundary condition is clamped-free. The first seventh frequencies and loss factors are reported in Table 2. Figure 3 represents the vibration spectrum displacement amplitude at the free end of the beam. For each mode, resonant frequencies and loss factors are determined. The damping is computed by the half power bandwidth method which remains accurate for low damping values [58].

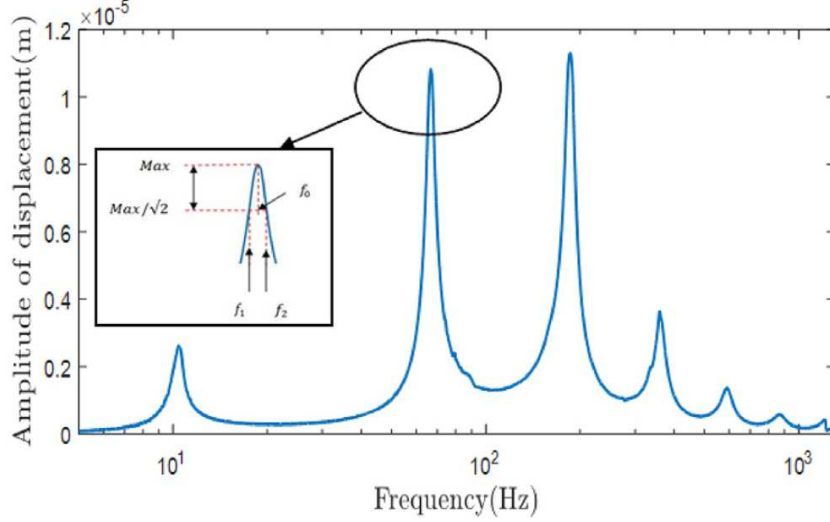


Figure 3: Spectrum of vibration displacement amplitude at the beam's free extremity

Table 2: Experimental modal data (frequencies are in Hz)

$f_1^{exp}$	$f_2^{exp}$	$f_3^{exp}$	$f_4^{exp}$	$f_5^{exp}$	$f_6^{exp}$	$f_7^{exp}$
11.03	69.33	193.27	376.72	614.84	910.08	1209.9
$\eta_1^{exp}$	$\eta_2^{exp}$	$\eta_3^{exp}$	$\eta_4^{exp}$	$\eta_5^{exp}$	$\eta_6^{exp}$	$\eta_7^{exp}$
0.075	0.057	0.054	0.0603	0.064	0.078	0.025

#### 200 4.2. Objective function

Let us denote by  $(f_i, \eta_i)$  the resonant frequencies and the loss factors. The identification strategy adopted here is to find the values of the viscoelastic complex modulus for each value of the resonant frequencies and then to perform interpolation on these values in order to obtain a continuous description of the shear complex modulus and loss factor over a wide range of frequencies. Let us set  $\omega_i^2 = (2\pi f_i)^2(1 + i\eta_i)$ . Since  
205  $(f_i, \eta_i)$  are resonant modal data for mode  $i$ , they are supposed to solve the non linear eigenvalue problem (36) derived from the finite element model described in section 2. If we write  $G^*(\omega_i) = G_i(1 + i\eta_i)$ , we obtain that for each mode  $\mathbf{U}_i$

$$\mathbf{T}(\lambda, G_i, \eta^i) = 0, \quad (56)$$

$$(\mathbf{K}_0 + G_i(1 + i\eta^i)\mathbf{K}_v - \omega_i^2\mathbf{M})\mathbf{U}_i = 0, \quad (57)$$

$$(58)$$

which means that once  $G_i$  and  $\eta^i$  are given,  $\omega_i$  and hence  $f_i$  and  $\eta_i$  could be found by solving a generalized standard eigenvalue problem in the complex domain. Thus, we can think of getting the values of  $G_i$  and  $\eta^i$  by minimizing an error between the numerically computed frequencies  $f_i^{num}$  and loss factors  $\eta_i^{num}$  and the experimental ones denoted by  $f_i^{exp}$  and  $\eta_i^{exp}$ . The error between numerical and experimental values can be defined for each mode  $i$  as follows:

$$\mathcal{J}(G_i, \eta^i) = w_1 \left( \frac{f_i^{num} - f_i^{exp}}{f_i^{exp}} \right)^2 + w_2 \left( \frac{\eta_i^{num} - \eta_i^{exp}}{\eta_i^{exp}} \right)^2. \quad (59)$$

### 4.3. Gradient validation

The gradient of the objective function  $\mathcal{J}$  versus  $(G_i, \eta^i)$  is computed by the adjoint approach described in section 3. Since  $f_i^{num} = \frac{\sqrt{\lambda_1^i}}{2\pi}$  and  $\eta_i^{num} = \frac{\lambda_2^i}{\lambda_1^i}$ , some quantities needed for the evaluation of the adjoint variables (see (52)) are given by:

$$\begin{aligned} \frac{\partial \mathcal{J}}{\partial \lambda_1^i} &= 2w_1 \frac{f_i^{num} - f_i^{exp}}{(f_i^{exp})^2} \frac{1}{8\pi^2 f_i^{num}} - 2w_2 \left( \frac{\eta_i^{num} - \eta_i^{exp}}{(\eta_i^{exp})^2} \frac{\eta_i^{num}}{4\pi^2 (f_i^{num})^2} \right), \\ \frac{\partial \mathcal{J}}{\partial \lambda_2^i} &= w_2 \frac{\eta_i^{num} - \eta_i^{exp}}{(\eta_i^{exp})^2} \frac{1}{4\pi^2 (f_i^{num})^2}, \\ \frac{\partial \mathcal{J}}{\partial \mathbf{x}_1} &= 0, \\ \frac{\partial \mathcal{J}}{\partial \mathbf{x}_2} &= 0. \end{aligned}$$

The evaluation of the gradient by (55) necessitates also the following quantities:

$$\begin{aligned} \frac{\partial \mathbf{T}}{\partial G_i} &= (1 + i\eta^i) \mathbf{K}_v, \\ \frac{\partial \mathbf{T}}{\partial \eta^i} &= iG_i \mathbf{K}_v. \end{aligned}$$

This adjoint gradient is compared to a central finite difference approach for the first four modes. We choose  $w_1 = w_2 = 0.5$ , a perturbation step of  $10^{-6}$  for the central difference scheme and compute the gradient with the two approaches for values of  $G_i$  from  $10^7$  to  $10^9$  (normalized between 0 and 1) and for  $\eta^i$  from 0 to 1. One can see from Figures 4-7 that the gradient provided by the adjoint approach is quite close to the gradient computed by finite differences which validates the adjoint approach.

## 5. Numerical examples

### 5.1. Use case 1

In this use case, modal data (see Table 4) is generated by solving (36) for the previous viscoelastic beam (see Table 1) under clamped-free boundary conditions, with a known shear complex viscoelastic modulus given by

$$G^*(\omega) = G_0 \left( 1 + \sum_{j=1}^{j=5} \frac{\delta_j \omega}{\omega - i\Omega_j} \right), \quad (60)$$

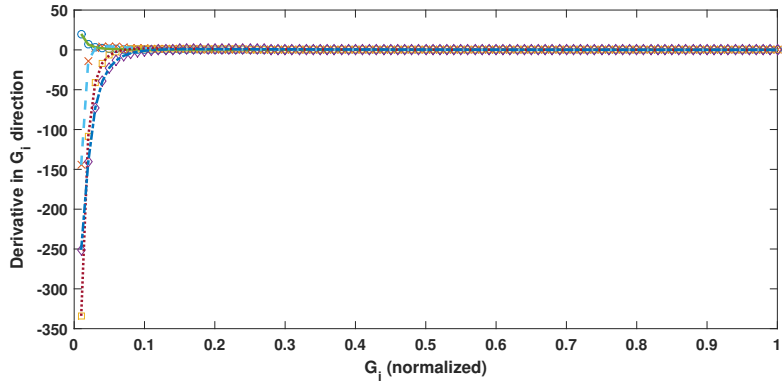


Figure 4: Derivative  $\frac{\partial \mathcal{J}}{\partial G_i}$  versus  $G_i$  (normalized between 0 and 1) for  $i = 1, \dots, 4$  by adjoint approach (Mode 1:  $\circ$ , Mode 2:  $\times$ , Mode 3:  $\square$ , Mode 4:  $\diamond$ ) and central finite differences (Mode 1:  $-$ , Mode 2:  $-$ , Mode 3:  $\dots$ , Mode 4:  $-$ ) for  $\eta^i = 0.5$

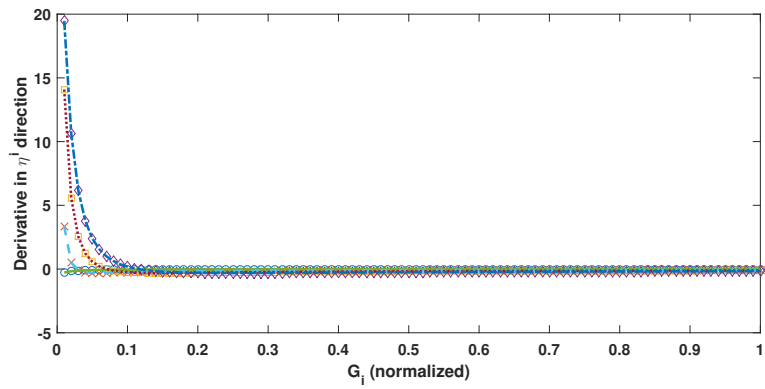


Figure 5: Derivative  $\frac{\partial \mathcal{J}}{\partial \eta^i}$  versus  $G_i$  (normalized between 0 and 1) for  $i = 1, \dots, 4$  by adjoint approach (Mode 1:  $\circ$ , Mode 2:  $\times$ , Mode 3:  $\square$ , Mode 4:  $\diamond$ ) and central finite differences (Mode 1:  $-$ , Mode 2:  $-$ , Mode 3:  $\dots$ , Mode 4:  $-$ ) for  $\eta^i = 0.5$

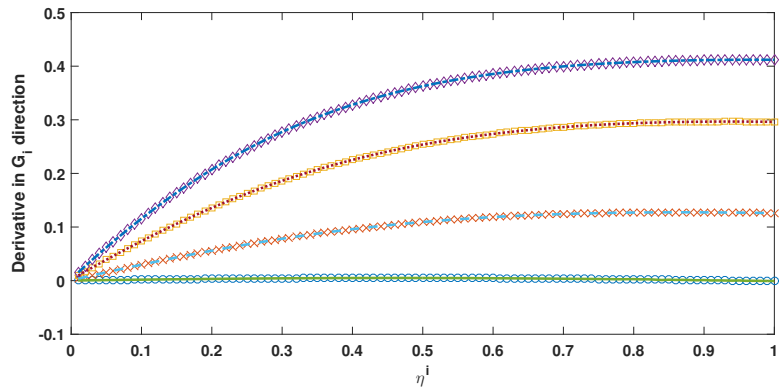


Figure 6: Derivative  $\frac{\partial \mathcal{J}}{\partial G_i}$  versus  $\eta^i$  for  $i = 1, \dots, 4$  by adjoint approach (Mode 1:  $\circ$ , Mode 2:  $\times$ , Mode 3:  $\square$ , Mode 4:  $\diamond$ ) and central finite differences (Mode 1:  $-$ , Mode 2:  $-$ , Mode 3:  $\dots$ , Mode 4:  $-$ ) for  $G_i = 0.5 \cdot 10^9$

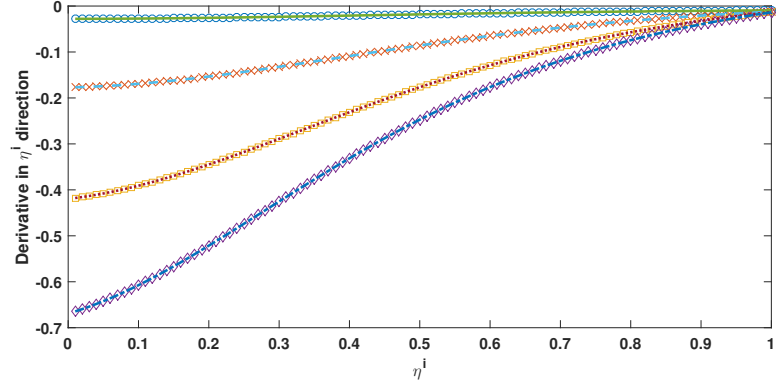


Figure 7: Derivative  $\frac{\partial \mathcal{L}}{\partial \eta^i}$  versus  $\eta^i$  for  $i = 1, \dots, 4$  by adjoint approach (Mode 1:  $\circ$ , Mode 2:  $\times$ , Mode 3:  $\square$ , Mode 4:  $\diamond$ ) and central finite differences (Mode 1:  $-$ , Mode 2:  $-$ , Mode 3:  $-$ , Mode 4:  $-$ ) for  $G_i = 0.5 \cdot 10^9$

Table 3: Fit parameters

$j$	$\delta_j$	$\Omega_j(\text{rad/s})$
1	1.3545	12.4547
2	3.2610	73.8749
3	7.7741	387.4302
4	18.9495	1472.7588
5	49.7732	9791.3957

Table 4: Numerically generated modal data (frequencies are in Hz)

$f_1$	$f_2$	$f_3$	$f_4$	$f_5$	$f_6$	$f_7$
6.606	31.2	77.4	141.4	225.2	326.4	445.8
$\eta_1$	$\eta_2$	$\eta_3$	$\eta_4$	$\eta_5$	$\eta_6$	$\eta_7$
0.52	0.44	0.405	0.31	0.23	0.18	0.14

220 with  $G_0 = 0.5 \cdot 10^6$  Pa and fit parameters  $(\delta_j, \Omega_j)$  given in Table 3. The optimization problem is solved thanks to a gradient based interior point algorithm used in the function *fmincon* of Matlab with a termination tolerance of  $10^{-12}$  on function values and  $10^{-10}$  on the optimization variables. The search space is fixed to  $[0, 10^6] \times [0, 2]$  for the couple  $(G_i, \eta^i)$ . The identified values are compared to the true values given by (60) as shown on Figures 8 for  $G_i$  and 9 for  $\eta^i$ . As one can see, the identified values match perfectly the 225 true values of the complex shear modulus used to generate the modal data which validates the identification process.

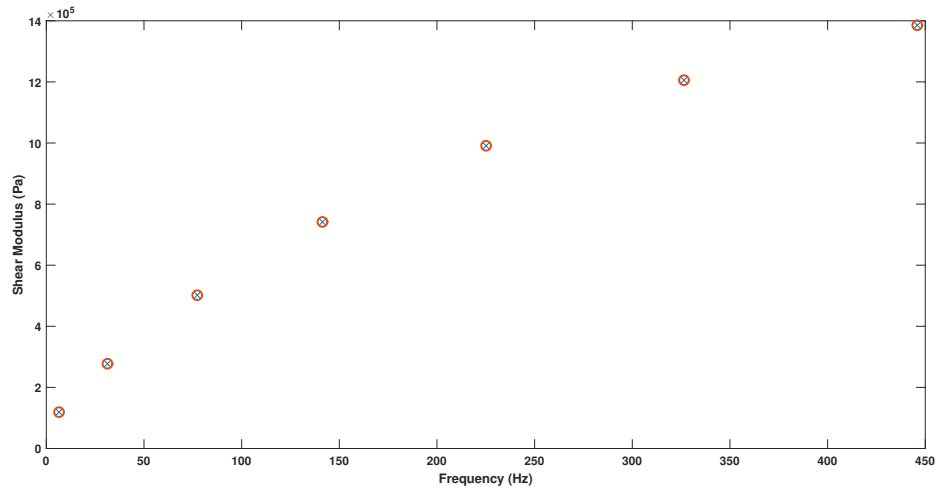


Figure 8: Identified and true values of the shear modulus  $G_i$  versus the frequency. Identified  $\circ$  and True  $\times$

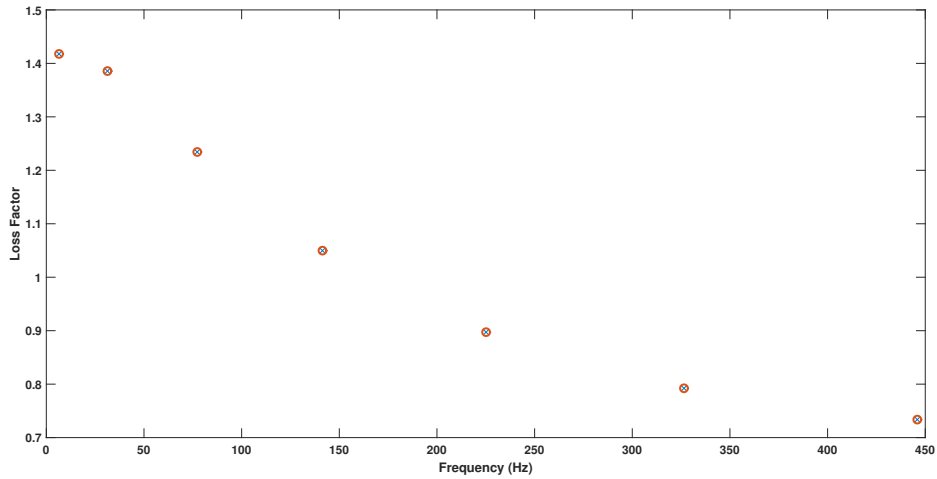


Figure 9: Identified and true values of the material loss factor  $\eta^i$  versus the frequency. Identified  $\circ$  and True  $\times$

## 5.2. Use case 2

Our goal is to identify the shear modulus and the loss factor of the viscoelastic beam using the experimental data presented in Table 2. In this case, we have no hint on the true complex shear modulus as in the

230 previous example. The search space is fixed to  $[0, 10^9] \times [0, 2]$  for the couple  $(G_i, \eta^i)$ . The optimization problem is solved thanks to a multistart strategy with 10 runs implemented via the function *ms* of Matlab. The interior point algorithm available through the generic function *fmincon* is used once again with the previous termination tolerances. This use case is more difficult than the first one since we have no hints on the true values and then we cannot check for convergence. Since gradient based methods are local methods, they need to be initialized with points near the optimum to converge. In the multistart strategy, the initial point is varied in such a way that the search is the most exhaustive possible. We adopted this strategy in order to increase our chances to find the the true value. The identified values of material shear modulus and loss factor are depicted in Figures 10 and 11, respectively. We notice that, the shear modulus becomes quasi frequency independent for frequencies higher than 950 Hz. It seems that for this viscoelastic material, the shear modulus approaches its maximal value while the loss factor reaches its minimal value. From the knowledge of typical evolutions of shear modulus and loss factors it can be inferred that the polymer is in the glassy regime above this frequency. The frequencies and loss factors obtained for the identified shear

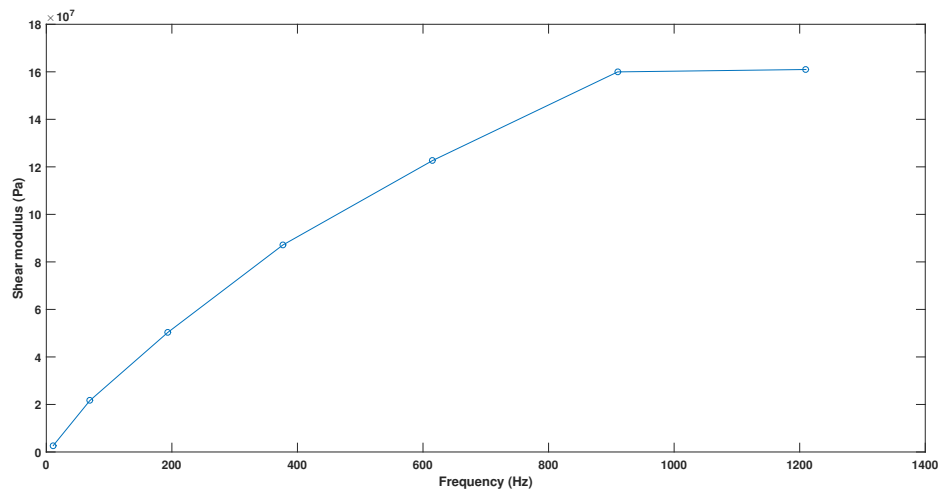


Figure 10: Identified values of the material shear modulus  $G_i$  versus the frequency.

modulus and loss factor are displayed in Table 5 . One can notice by comparison with Table 2 that the numerical modal characteristics are the same as for the experimental ones. It is worth noting that with the identified values of shear moduli and loss factors for each resonant frequency, the numerical and experimental values match. This means that the multistart gradient-based optimization strategy, used here, has been successful at minimizing the quadratic loss error (see (59)) between the experimental data and the numerical model. This error is for most of the modes near zero which explains that the experimental and numerical values of frequencies and loss factors are the same.

## 250 6. Conclusion

In the context of a non linear complex eigenvalue problem, a discrete adjoint method for gradient computation is derived. First, it is demonstrated that the method gives accurate results in comparison with

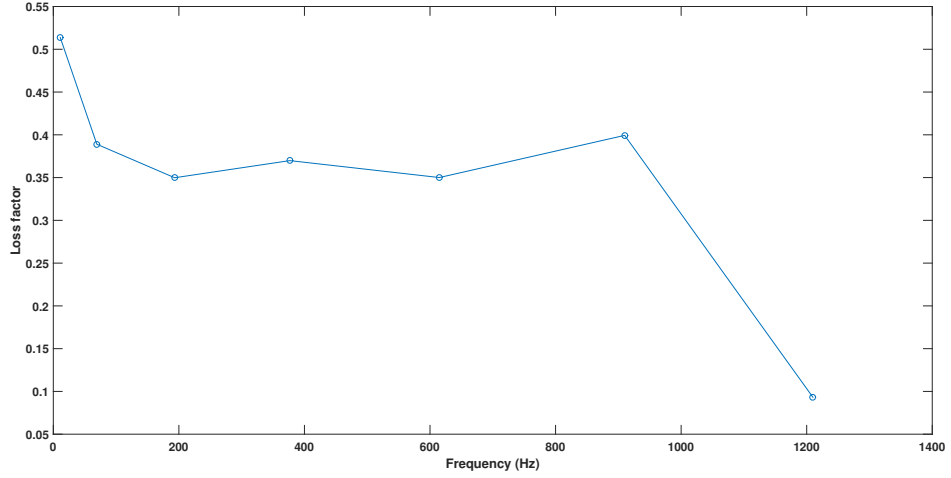


Figure 11: Identified values of the material loss factor  $\eta^i$  versus the frequency.

Table 5: Identified modal characteristics (frequencies are in Hz)

$f_1^{num}$	$f_2^{num}$	$f_3^{num}$	$f_4^{num}$	$f_5^{num}$	$f_6^{num}$	$f_7^{num}$
11.03	69.329	193.27	376.72	614.84	910.08	1209.9
$\eta_1^{num}$	$\eta_2^{num}$	$\eta_3^{num}$	$\eta_4^{num}$	$\eta_5^{num}$	$\eta_6^{num}$	$\eta_7^{num}$
0.0749	0.0569	0.054	0.0602	0.064	0.078	0.025

central finite difference schemes. Then, the validated method is applied to the identification of the complex shear modulus of a viscoelastic sandwich beam using modal data. In a first use case, it is shown that the method is able to identify with accuracy the values of shear modulus and loss factor of a known viscoelastic material. Then, in a second use case the method is applied to real modal data stemming from vibration tests to identify the shear and the loss factor of a real viscoelastic material. These different tests show the ability of the adjoint gradient approach to solve optimization based identification problems.

## Acknowledgements

This work was supported by the French State through the program “Investment in the future” operated by the National Research Agency (ANR) and referenced by ANR-11-LABX-0008-01 (LabEx DAMAS).

## References

- [1] D. K. Rao, Frequency and loss factors of sandwich beams under various boundary conditions, *Journal of Mechanical Engineering Science* 20 (5) (1978) 271–282. arXiv:<http://jms.sagepub.com/content/20/5/271.full.pdf+html>, doi:10.1243/JMES\_JOUR\_1978\_020\_047\_02.

- [2] M. L. Soni, Finite element analysis of viscoelastically damped sandwich structures, *Shock and Vibration Bulletin* 55 (1) (1981) 97–109.
- [3] C. D. Johnson, D. A. Kienholz, Finite element prediction of damping in structures with constrained viscoelastic layers, *American Institute of Aeronautics and Astronautics* 20 (9) (1982) 1284–1290.
- 270 [4] B.-A. Ma, J.-F. He, A finite element analysis of viscoelastically damped sandwich plates, *Journal of Sound and Vibration* 152 (1) (1992) 107–123.
- [5] E. M. Daya, M. Potier-Ferry, A shell finite element for viscoelastically damped sandwich structures, *European Journal of Computational Mechanics* 11 (1) (2002) 39–56.
- 275 [6] X. Chen, H. Chen, X. Hu, Damping prediction of sandwich structures by order-reduction-iteration approach, *Journal of Sound and Vibration* 222 (5) (1999) 803–812.
- [7] M. Bilasse, L. Azrar, E. Daya, Complex modes based numerical analysis of viscoelastic sandwich plates vibrations, *Computers & Structures* 89 (7-8) (2011) 539 – 555. doi:http://dx.doi.org/10.1016/j.compstruc.2011.01.020.
- 280 [8] J. Moita, A. Araujo, P. Martins, C. M. Soares, C. M. Soares, A finite element model for the analysis of viscoelastic sandwich structures, *Computers & Structures* 89 (21-22) (2011) 1874 – 1881. doi:http://dx.doi.org/10.1016/j.compstruc.2011.05.008.
- [9] K. Akoussan, H. Boudaoud, E. M. Daya, E. Carrera, Vibration modeling of multilayers composite structures with viscoelastic layers, *Mechanics of Advanced Materials and Structures* 0 (ja) (0) 00–00. doi:10.1080/15376494.2014.907951.
- 285 [10] S. Zghal, M. L. Bouazizi, N. Bouhaddi, R. Nasri, Model reduction methods for viscoelastic sandwich structures in frequency and time domains, *Finite Elements in Analysis and Design* 93 (2015) 12 – 29. doi:https://doi.org/10.1016/j.finel.2014.08.003.
- [11] F. J. D., *Viscoelastic properties of polymers*, John Wiley & Sons, 1980.
- 290 [12] G. L., S. A., Parameter identification and fe implementation of a viscoelastic constitutive equation using fractional derivatives., *PAMM (Proc Appl Math Mech)* 1 (1) (2002) 153–154.
- [13] S. Gerlach, A. Matzenmiller, Comparison of numerical methods for identification of viscoelastic line spectra from static test data, *International journal for numerical methods in engineering* 63 (3) (2005) 428–454.
- 295 [14] R. Lewandowski, B. Chorazyczewski, Identification of the parameters of the kelvin–voigt and the maxwell fractional models, used to modeling of viscoelastic dampers, *Computers & Structures* 88 (1) (2010) 1 – 17.
- [15] K. P. Menard, *Dynamic Mechanical Analysis: A Practical Introduction*, CRC Press, 1999.

- [16] J. Landier, Modélisation et étude expérimentale des propriétés amortissantes des tôles sandwich, Ph.D. thesis, University of Metz (1993).
- [17] N. Makris, Complex-parameter Kelvin model for elastic foundations, *Earthquake engineering and structural dynamics* 23 (3) (1994) 251–264.
- [18] M. Soula, T. Vinh, Y. Chevalier, Transient responses of polymers and elastomers deduced from harmonic responses, *Journal of Sound and Vibration* 205 (2) (1997) 185 – 203.
- [19] T. Pritz, Five-parameter fractional derivative model for polymeric damping materials, *Journal of Sound and Vibration* 265 (5) (2003) 935 – 952.
- [20] T. Beda, Y. Chevalier, New methods for identifying rheological parameter for fractional derivative modeling of viscoelastic behavior, *Mechanics of Time-Dependent Materials* 8 (2) (2004) 105–118.
- [21] F. Renaud, J.-L. Dion, G. Chevallier, Méthode d’identification des paramètres d’un modèle de maxwell généralisé pour la modélisation de l’amortissement, *Mechanics & Industry* 11 (1) (2010) 47–55.
- [22] L. Rouleau, J.-F. Deü, A. Legay, F. L. Lay, Application of kramers–kronig relations to time–temperature superposition for viscoelastic materials, *Mechanics of Materials* 65 (2013) 66 – 75.
- [23] A. International, Astm e756-05 - standard test method for measuring vibration-damping properties of materials, Tech. rep., ASTM International (2010).
- [24] D. D. Ewins, Modal analysis - Theory and Practice, 2nd Edition, Mechanical engineering research studies, Research studies press Ltd, 1984.
- [25] D. Ross, E. E. Ungar, E. M. Kerwin, Damping of plate flexural vibrations by means of viscoelastic laminae, in: J. E. Ruzicka (Ed.), *Structural Damping*, Pergamon Press, Oxford, 1960, pp. 49–87.
- [26] F. S. Barbosa, M. C. R. Farage, A finite element model for sandwich viscoelastic beams: Experimental and numerical assessment, *Journal of Sound and Vibration* 317 (1-2) (2008) 91–111.
- [27] S.-Y. Kim, D.-H. Lee, Identification of fractional-derivative-model parameters of viscoelastic materials from measured frfs, *Journal of Sound and Vibration* 324 (3) (2009) 570 – 586.
- [28] E. Barkanov, E. Skukis, B. Petitjean, Characterisation of viscoelastic layers in sandwich panels via an inverse technique, *Journal of Sound and Vibration* 327 (3) (2009) 402 – 412.
- [29] I. Elkhaldi, I. Charpentier, E. M. Daya, A gradient method for viscoelastic behaviour identification of damped sandwich structures, *Comptes Rendus Mécanique* 340 (8) (2012) 619 – 623.
- [30] M. Martinez-Agirre, M. Jesus Elejabarrieta, Dynamic characterization of high damping viscoelastic materials from vibration test data, *Journal of Sound and Vibration* 330 (16) (2011) 3930–3943. doi: {10.1016/j.jsv.2011.03.025}.

- [31] T. Wassereau, F. Ablitzer, C. Pezerat, J.-L. Guyader, Experimental identification of flexural and shear complex moduli by inverting the Timoshenko beam problem, *Journal of Sound and Vibration* 399 (2017) 86–103. doi:{10.1016/j.jsv.2017.03.017}.
- [32] W. Sun, Z. Wang, X. Yan, M. Zhu, Inverse identification of the frequency-dependent mechanical parameters of viscoelastic materials based on the measured FRFs, *Mechanical Systems And Signal Processing* 98 (2018) 816–833. doi:{10.1016/j.ymsp.2017.05.031}.
- [33] K. Ledi, M. Hamdaoui, G. Robin, E. Daya, An identification method for frequency dependent material properties of viscoelastic sandwich structures, *Journal of Sound and Vibration* 428 (2018) 13 – 25. doi:https://doi.org/10.1016/j.jsv.2018.04.031.
- [34] M. Bilasse, E. Daya, L. Azrar, Linear and nonlinear vibrations analysis of viscoelastic sandwich beams, *Journal of Sound and Vibration* 329 (23) (2010) 4950 – 4969.
- [35] J. E. Peter, R. P. Dwight, Numerical sensitivity analysis for aerodynamic optimization: A survey of approaches, *Computers & Fluids* 39 (3) (2010) 373 – 391. doi:https://doi.org/10.1016/j.compfluid.2009.09.013.
- [36] J. Ringuest, Substitute derivatives in unconstrained optimization - A comparison of finite-difference and response surface approximations, *Computers & Operations Research* 15 (4) (1988) 341–352. doi:{10.1016/0305-0548(88)90018-4}.
- [37] J. Martins, P. Sturdza, J. Alonso, The complex-step derivative approximation, *ACM Transactions on Mathematical Software* 29 (3) (2003) 245–262. doi:{10.1145/838250.838251}.
- [38] A. Griewank, A. Walther, Evaluating Derivatives: Principles and Techniques of Algorithmic Differentiation, Second Edition, in: *Evaluating derivatives: principles and techniques of algorithmic differentiation, second edition*, Vol. 105 of *Other Titles in Applied Mathematics*, SIAM, 2008, pp. 1–438. doi:{10.1137/1.9780898717761}.
- [39] M. Gunzburger, Sensitivities, adjoints and flow optimization, *International Journal for numerical methods in fluids* 31 (1) (1999) 53–78.
- [40] K. R.E., Contributions to the theory of optimal control, *Boletin de la Sociedad Matematica Mexicana* 5 (32) (1960) 102–109.
- [41] L. Pontryagin, V. Boltyanskij, R. Gamkrelidze, E. Mishchenko, The mathematical theory of optimal processes. Translated from the Russian by D.E.Brown., *International Series of Monographs on Pure and Applied Mathematics.*, Pergamon Press. VII, 1964.
- [42] J.-L. Lions, *Optimal Control of Systems Governed by Partial Differential Equations*, Vol. 1 of *Grundlehren der mathematischen Wissenschaften*, Springer-Verlag, 1971.

- [43] X. Qian, E. M. Dede, Topology optimization of a coupled thermal-fluid system under a tangential thermal gradient constraint, *Structural and Multidisciplinary Optimization* 54 (3) (2016) 531–551.
- 365 [44] J. S. Jensen, P. B. Nakshatrala, D. A. Tortorelli, On the consistency of adjoint sensitivity analysis for structural optimization of linear dynamic problems, *Structural and Multidisciplinary Optimization* 49 (5) (2014) 831–837.
- [45] R. Troian, F. Gillot, S. Besset, Adjoint sensitivity related to geometric parameters for mid-high frequency range vibroacoustics, *Structural and Multidisciplinary Optimization* 52 (4) (2015) 803–811.
- 370 [46] M. B. Giles, N. A. Pierce, An introduction to the adjoint approach to design, *Flow, Turbulence and Combustion* 65 (3) (2000) 393–415.
- [47] R. Joslin, M. Gunzburger, R. Nicolaides, G. Erlebacher, M. Hussaini, Self-contained automated methodology for optimal flow control, *AIAA Journal* 35 (5) (1997) 816–824.
- [48] Z. Mróz, A. Garstecki, Optimal loading conditions in the design and identification of structures. part 375 1: discrete formulation, *Structural and Multidisciplinary Optimization* 29 (1) (2005) 1–18.
- [49] R. E. Plessix, A review of the adjoint-state method for computing the gradient of a functional with geophysical applications, *Geophysical Journal International* 167 (2) (2006) 495–503. doi: {10.1111/j.1365-246X.2006.02978.x}.
- 380 [50] J. Degroote, M. Hojjat, E. Stavropoulou, R. Wüchner, K.-U. Bletzinger, Partitioned solution of an unsteady adjoint for strongly coupled fluid-structure interactions and application to parameter identification of a one-dimensional problem, *Structural and Multidisciplinary Optimization* 47 (1) (2013) 77–94.
- [51] H. Hu, S. Belouettar, M. Potier-Ferry, E. M. Daya, Review and assessment of various theories for modeling sandwich composites, *Composite Structures* 84 (3) (2008) 282 – 292. 385 doi: <http://dx.doi.org/10.1016/j.compstruct.2007.08.007>.
- [52] E. M. Daya, M. Potier-Ferry, A numerical method for nonlinear eigenvalue problems application to vibrations of viscoelastic structures, *Computers & Structures* 79 (5) (2001) 533–541.
- [53] M. Martinez-Agirre, M. J. Elejabarrieta, Higher order eigensensitivities-based numerical method for the harmonic analysis of viscoelastically damped structures, *International Journal for numerical methods in engineering* 88 (12) (2011) 1280–1296. 390
- [54] K. Schreiber, Nonlinear eigenvalue problems: Newton-type methods and nonlinear rayleigh functionals, Ph.D. thesis, Technischen Universität Berlin (2008).
- [55] H. Voss, An Arnoldi method for nonlinear eigenvalue problems, *BIT Numerical Mathematics* 44 (2004) 387 – 401.

- 395 [56] H. Voss, A Jacobi–Davidson method for nonlinear and nonsymmetric eigenproblems, *Computers & Structures* 85 (2007) 1284 – 1292.
- [57] M. Hamdaoui, K. Akoussan, E. M. Daya, Comparison of non-linear eigensolvers for modal analysis of frequency dependent laminated visco-elastic sandwich plates, *Finite Elements in Analysis and Design* 121 (Supplement C) (2016) 75 – 85.
- 400 [58] A. K. Chopra, *Dynamics of Structures: Theory and Applications to Earthquake Engineering*, 5th Edition, Pearson, 2017.